Pertanika J. Sci. & Technol. 26 (1): 85 - 94 (2018)

SCIENCE & TECHNOLOGY

Journal homepage: http://www.pertanika.upm.edu.my/

The Simulation of a Force in Micro-scale Sensing Employing an Optical Double Ring Resonator System

Youplao, P.[1]*, Tasakorn, M.[1] and Phattaraworamet, T.[2]

[1]Department of Electrical Engineering, Faculty of Industry and Technology, Rajamangala University of Technology Isan Sakon Nakhon Campus, Sakon Nakhon 47160, Thailand
[2]Department of Electrical and Computer Engineering, Faculty of Science and Engineering, Kasetsart University, Chalermphrakiat Sakon Nakhon Province Campus, Sakon Nakhon 47000, Thailand

ABSTRACT

This paper presents an optical double-ring resonator system of which the design and analytical model are demonstrated to be useful as a novel force in micro-Newton measurement-sensing devices based on optical sensors. The sensing application can be accomplished by changing the optical filtering characteristic of an optical resonance structure such as the ring resonator system. Together with the concept of stress/strain and the elastic modulus of the waveguide material, the relationship between a slightly different value in the exerted force acting on the sensing unit and a difference in the waveguide length can be evaluated. Indeed, changing the optical path length (the waveguide length) causes the difference in peak spectrum of the filtering signals obtained from a ring resonator system. Hence, by measuring the spacing shift between the sensing and setting peak signal in the considered channel, the measurement of a slightly different value in the exerted forces on the sensing unit can be achieved. From the simulation results, an exerted force in small-scale ranges from 10 μN to 50 μN have been evaluated by measuring a spacing shift between the peak signals ranging from 35 pm to 225 pm. In this study, the potential of using such a double-ring resonator device for a force in micro-Newton sensing application is studied and discussed.

Keywords: Force sensing, optical sensors, optical resonance, optical filter, ring resonator

INTRODUCTION

Force sensing is crucial especially in micro-manipulation for monitoring mechanical behaviour or generating feedback signals for robotic systems in order to execute reliable operations and avoid damaging fragile objects such as the micro-force sensor used in minimally invasive surgery (Peirs et al., 2004; Baki et al., 2012; Abushagur et al., 2014). In

ARTICLE INFO

Article history:
Received: 02 June 2016
Accepted: 07 November 2017

E-mail addresses:
phichai.yo@rmuti.ac.th (Youplao, P.),
mtasakorn@yahoo.fr (Tasakorn, M.),
thanawat.pha@ku.th (Phattaraworamet, T.)
*Corresponding Author

ISSN: 0128-7680

addition, when manipulating biological cells, encountered forces are typically found in micro-Newton measurement, which the sensing devices use through microfabrication techniques. Various research methods in this field have been used such as the design and fabrication of a force sensor based on silicon micro-machining technology (Jin & Mote, 1998; Cappelleri et al., 2011), magnetic resonance imaging as a fibre-optic force sensor (Tokuno et al., 2008; Marchi et al., 2016), a microfiber-coupler-based reflective sensor, fabricated by fusing two twisted optical fibres and then connecting the two ends to form a Sagnac loop (Chen et al., 2014) and a parallel plate structure (Tan et al., 2011). Some methods used indirect measurement techniques as capacitance-based force measurement (Enikov & Nelson, 2000), with many micromachining steps of fabrication work (Zadeh et al., 2017). The piezo-resistive cantilever force measurement technique has also been used through electrical conversion of small gauges (Beyeler et al., 2007; Li et al., 2009; Alcheikh et al., 2013; Caseiro et al., 2014) and by using a composite material consisting of a conductive ink and silicon elastomer (Cho & Ryuh, 2016). However, the implementation of these measurement methods are difficult to conduct in micro-electromechanical systems due to complications in using the devices and the fabrication costs.

Ring resonators have been receiving extensive attention as useful micro-components, without any unnecessary electronic parts, in optical systems. Many of the potential applications have been investigated and proposed, such as optical logic gate operators (Bao et al., 2014; Rakshit & Roy, 2014), optical switch (Yan et al., 2010), nonlinear signal processing (Dumeige et al., 2005; Yupapin & Suwancharoen, 2007) and optical filters (Yang et al., 2003; Liua et al., 2007; Ma & Ogusu, 2011). In this paper, the design and simulation results of the proposed system consisting of two micro-ring resonators to be used as a force-sensing device are presented. The potential of using such a proposed system for measuring force in micro-scale levels is also examined and discussed.

THE PROPOSED RING RESONATOR SYSTEM

The proposed ring resonator system, of which the schematic diagram is shown in Figure 1, is employed as a micro-force sensing device. The system consists of two ring resonators, R_1 with an optical input port, and R_2 as a sensing unit with an optical drop port. In operation, a Gaussian light pulse from a monochromatic light source is used as the optical input signal that launches the system. The input signal is considered a function that consists of a constant light field amplitude, E_0, and random phase modulation, which is the combination of an attenuation, α, and a phase constant, ϕ_0, resulting in temporal coherence degradation. In the equation where L is the propagation distance, the time-dependent input optical field, $E_{in}(t)$, can be expressed as:

$$E_{in}(t) = E_0 \exp\left[-\alpha L + j\phi_0(t)\right] \quad [1]$$

When the Gaussian pulse is propagating through the ring resonator system, in the direction shown in Figure 1, the resonant optical fields are formed and then appear separately at the

throughput port and drop port of the system, which are represented by E_{th} and E_{drop}, respectively. The relations between each optical field output, E_{th} or E_{drop}, and the optical field input, E_{in}, in each round trip calculation can be expressed as:

$$\left|\frac{E_{th}}{E_{in}}\right|^2 = \frac{(1-\kappa_1)y_1^2 - 2x_1x_2y_1\sqrt{1-\kappa_1}e^{-\frac{\alpha}{2}L_1}\cos(knL_1) + y_1y_2e^{-\alpha L_1}}{y_1^2 - 2x_1x_2y_1\sqrt{1-\kappa_1}e^{-\frac{\alpha}{2}L_1}\cos(knL_1) + (1-\kappa_1)y_1y_2e^{-\alpha L_1}} \quad [2]$$

$$\left|\frac{E_{drop}}{E_{in}}\right|^2 = \frac{y_1\kappa_1\kappa_2\kappa_3e^{-\frac{\alpha}{2}(L_1+L_2)}}{y_1^2 - 2x_1x_2y_1\sqrt{1-\kappa_1}e^{-\frac{\alpha}{2}L_1}\cos(knL_1) + (1-\kappa_1)y_1y_2e^{-\alpha L_1}} \quad [3]$$

where, the optical field, E_i, propagates within each part, i, of the ring resonator system, as well described by Rabus (2002). The specified constant quantities of C_n, x_n and y_n are given in Table 1.

Table 1
Expression of optical field, $E_{(i)}$ and constant quantities of C_n, x_n and y_n

Optical Fields, E_i	Constant Quantities, C_n, x_n, y_n
$E_1 = E_{in}j\sqrt{\kappa_1} + E_4\sqrt{1-\kappa_1}e^{-\frac{\alpha L_1}{2}-jkn\frac{L_1}{2}}$	$C_1 = 1 - \sqrt{1-\kappa_2}\sqrt{1-\kappa_3}e^{-\frac{\alpha}{2}L_2-jknL_2}$
$E_2 = E_1j\sqrt{\kappa_2}e^{-\frac{\alpha L_1}{2}-jkn\frac{L_1}{2}} + E_3\sqrt{1-\kappa_2}e^{-\frac{\alpha L_2}{2}-jkn\frac{L_2}{2}}$	$C_2 = \sqrt{1-\kappa_2} - \sqrt{1-\kappa_3}e^{-\frac{\alpha}{2}L_2-jknL_2}$
$E_3 = E_2\sqrt{1-\kappa_3}e^{-\frac{\alpha L_2}{2}-jkn\frac{L_2}{2}}$	$x_n = \lvert C_n \rvert$
$E_4 = E_3j\sqrt{\kappa_2}e^{-\frac{\alpha L_2}{2}-jkn\frac{L_2}{2}} + E_1\sqrt{1-\kappa_2}e^{-\frac{\alpha L_1}{2}-jkn\frac{L_1}{2}}$	$y_n = \lvert C_n \rvert^2$

Equations [2] and [3] indicate that the ring resonator system in this particular case is similar to a Fabry-Perot cavity, which consists of two parallel highly reflecting mirrors that function as a fully reflecting mirror, κ, and a field reflectivity, (1-κ), where κ is the coupling coefficient. The details of the specific variables are as follows: the linear absorption coefficient is α, a roundtrip loss coefficient is $e^{-\alpha Li/2}$, the linear phase shift is $\phi_i = kn_i L_i$, the waveguide length of the ring radius R_i is $L_i = 2\pi R_i$ and n_i is the refractive index of the waveguide material of R_i.

In operation, the input optical field with a specified wavelength, E_{in}, i.e. a Gaussian pulse from a monochromatic light source, is launched into the proposed ring resonator system, of which the appropriate parameters, such as the radius of the rings (waveguide length) and the coupling coefficients, must be assigned so that the transmitted output signals can be controlled.

Figure 1 shows, in principle, while propagating within the ring system, the input light pulse is divided and sliced as the discrete signal by the first ring, R_1, and then spread to the another ring, R_2, with the direction as shown in the figure. Finally, the required signals are obtained separately via the throughput port and the drop port of the ring system.

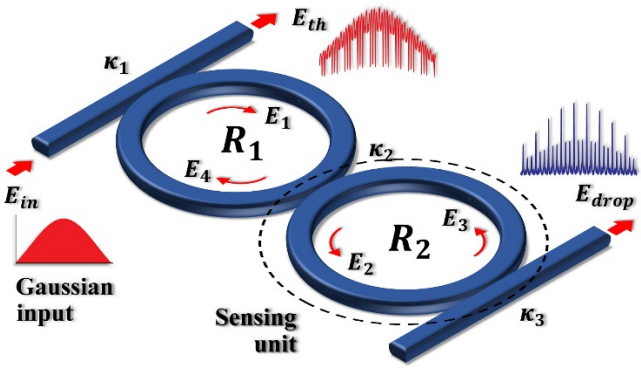

Figure 1. Schematic diagram of the proposed ring resonator system

SIMULATION RESULTS

Normally, the optical Vernier effects, which have a potential for use in high-resolution distance measurement, can be generated by using an optically resonant structure such as a micro-ring resonator (Boeck et al., 2010). A Gaussian input with a specified wavelength ranging from 1.545–1.555 μm (C-band), 10 nm bandwidth and a peak power of 0.2 W, can be propagated through the proposed system. Thereafter, the resonant outputs each at the throughput port and the drop port are obtained with the optical Vernier effects as shown in Figure 2. In this work, the ring resonator system is proposed to be useful as a force in a micro-scale sensing devices. Micro-sensing can be performed by measuring the spacing shift among the setting and sensing peak spectrum signals that are obtained from the drop port of the system. In order to associate the system with a practical device (Takara et al., 2002; Xu et al., 2004), the system parameters are specified as follows: the ring radius $R_1 = 300$ μm and the sensing unit ring $R_2 = 60$ μm. The refractive index of the waveguide material is fixed at n = 3.47 (Si–Crystalline silicon). The coupling coefficients, κ, of the system ranges from 0.10-0.20. The waveguide (ring system) loss is considered to be α= 0.5 dB/mm. For simplification, the optical field relation does not take into account the coupling losses (Rabus et al., 2002). In operation, the signal wavelength shift resolution in a nano-scale region within the interferometer ring R_2 can be achieved by changing its optical path length. For instance, the force exertion can be performed as a diffused force acting on the thin film, which is coated on the sensing unit; hence, the optical path length of the sensing unit within the thin film is also changed concurrently during the force exertion. The change in optical path length is related to the change in exerted force on the sensing unit, which is according to the stress/strain of the waveguide material. Finally, the setting and sensing signal are observed and compared to evaluate an amount of the exerted force on the sensing unit.

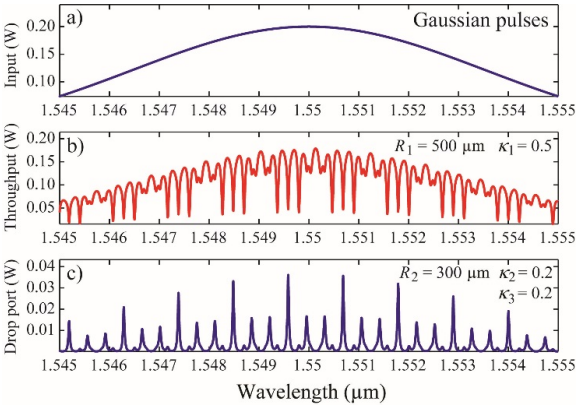

Figure 2. Simulation results with the obtained optical Vernier effects for a Gaussian pulse input of 10 nm bandwidth as a function of wavelength from 1.545 to 1.555 μm

The concept of stress and strain on the sensing unit by the elastic modulus of the waveguide material, which causes the difference in peak spectrum of the output signals, and the relationship between the exerted force and the change in waveguide length, can be expressed by equation [4] and [5], respectively.

$$Y_0 = \frac{Stress}{Strain} = \left(\frac{F}{A_0} \times \frac{L_0}{\Delta L}\right) \quad [4]$$

$$F = \left(\frac{Y_0 A_0}{L_0}\right) \times \Delta L \quad [5]$$

where, F is the exerted force in a small-scale ranging from 10 μN to 50 μN, Y_0 is Young's modulus of the waveguide material, which is approximately 160 kN/mm^2 for the Si–Crystalline silicon (Hopcroft et al., 2010). The initial cross-sectional area of the sensing unit waveguide is represented by A_0, which is specified as 0.054 μm^2, while L_0 is the initial waveguide length, which equals to $2\pi R_2$ μm, and ΔL is the change in waveguide length.

Figure 3 shows the simulation results of the proposed system as the setting spectrum signal (no force exertion) compared with each sensing spectrum signal, with the exerted force given as 10 μN, 20 μN, 30 μN, 40 μN and 50 μN, resulting in the changes in a spacing shift among the sensing and setting peak signal; this can be seen for instance in Channel 1 as approximately 35 pm, 72 pm, 110 pm, 149 pm and 189 pm, respectively.

Figure 4 shows the comparison between the setting and sensing spectrum signal in the other channels, Channel 2, Channel 3 and Channel 4, with the same mentioned conditions. The changes in spacing shift among the setting and sensing signal in each condition and channel are given by the figure.

By the well-known linear regression, with more than 99% of R^2, the linearity relations between the exerted forces and the free spectral range shifts of each considered channel, such as ch.1 to ch.4, have been illustrated as in Figure 5.

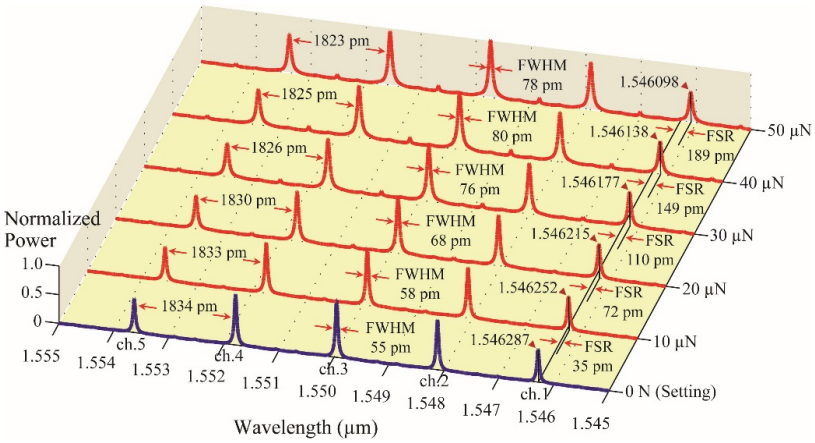

Figure 3. Simulation results of the comparing spectrum between the setting and sensing spectrum that can be obtained by the ring resonator system while exerting a force of 10 μN, 20 μN, 30 μN, 40 μN and 50 μN on the sensing unit

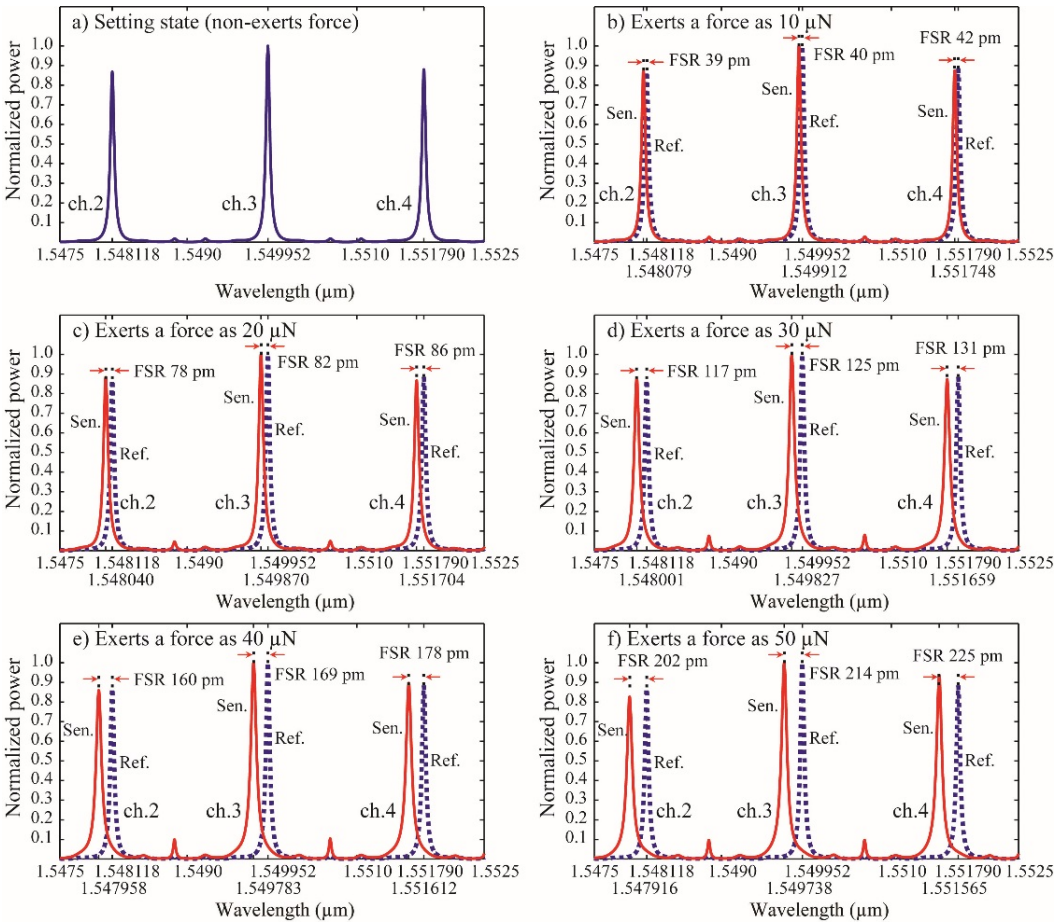

Figure 4. Simulation results of the comparing spectrum between the setting and sensing spectrum in channel 2, 3 and 4, a) for the setting state, b), c), d), e) and f), for a force exertion of 10 μN, 20 μN, 30 μN, 40 μN and 50 μN, respectively

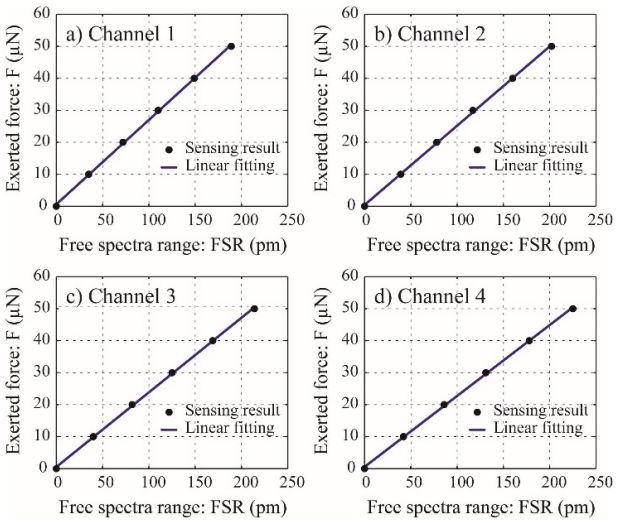

Figure 5. Linearity relation of the exerted forces as a function of free spectra range shifts in each considered channel

DISCUSSION

Although the proposed ring resonator system has the potential to be useful as a micro-force sensing device, there are significant uncertainties to be considered for its proper function. These uncertainties are listed below.

S1. Errors in the fabrication process: The proposed ring resonator system is designed to function within specific parameters, such as the ring radius, the coupling coefficients and the refractive index of the waveguide material. In practice, the resonant response of the ring resonator system needs to be customised for a particular device since the fabrication process may have some unavoidable errors in the required system parameters that would result in errors in the resonant outputs of the actual device. The most typical and straightforward approach for tuning the resonant response of a micro-ring resonator is to change the refractive index of the waveguide material, using perhaps the thermo-optic or electro-optic effect method, which applies the heat or electrical field to the waveguide (Prasad et al., 2016; Kim, 2015). The carrier injection method aims to change loss parameters and a refractive index of the material (Bulutay et al., 2010). The chemical method uses the chemical potential of graphene to tune the refractive index of the waveguides (Perez et al., 2016; Xing & Jian, 2017). Therefore, in order to function properly, the fabrication work must take into account the waveguide tuning techniques, which were not considered in this investigation.

S2. Elasticity of doped silicon: Generally, silicon wafers are not made of pure silicon, but usually have a certain amount of chemical impurities that are added to control the wafers' properties; this is called doping. The volume of the doping atoms on crystalline silicon is normally negligible but it may have an effect on the elastic behaviour of the waveguide.

However, the changes typically decrease by 1%-3% in heavy doping (Hopcroft et al., 2010); this percentage of doping can be neglected.

S3. Elasticity of thin film: As the force exertion is performed by a diffused force acting on the thin film, which is coated on the sensing unit, in practice, the change in the optical path length of the waveguide may also be influenced by the elasticity of the thin film. It is difficult to identify by how much the sensing results are exactly affected by the elasticity of the thin film since it can be made up of a variety of materials. However, the thin film could be made up of Low-Density Polyethylene (LDPE), which has a variety of applications in industry, of which Young's modulus is 150 N/mm^2 (Molaei, 2016), corresponding to 0.094% with respect to Young's modulus of the waveguide material (Si-Crystalline silicon), which can be neglected.

CONCLUSION

In this paper, an optical ring resonator system of which the resonant outputs were observed and compared to be useful as a force in a micro-scale sensing device was presented. The sensing application can be accomplished by evaluating the changes in the filtering characteristics together with the concept of stress/strain and the elastic modulus of the waveguide material. In operation, the force exertion can be performed as a diffused force acting within the thin film that is coated on the sensing unit, of which the optical path length can also be changed proportionally to the amount of the exerted force. From the simulation results, the exerted force ranged from 10 μN to 50 μN upon the sensing unit; this can be evaluated as the spacing shift between the setting and sensing peak signal of 35 pm to 225 pm. The sensing relation was obtained as good linearity, with more than 99% of R^2.

ACKNOWLEDGEMENT

We would like to express our thanks to Sakon Nakhon Rajabhat University International Conference 2015 (SNRU-IC 2015) for help in preparing this paper.

REFERENCES

Abushagur, A. A. G., Arsad, N., Reaz, M. I., & Bakar, A. A. A. (2014). Advances in bio-tactile sensors for minimally invasive surgery using the fibre Bragg grating force sensor technique: A survey. *Sensors, 14*(4), 6633-6665.

Alcheikh, N., Coutier, C., Giroud, S., Poulain, C., & Rey, P. (2013). Characterization and modeling of a piezoresistive three-axial force micro sensor. *Sensors and Actuators A: Physical, 201*, 188-192.

Baki, P., Szekely, G., & Kosa, G. (2012). Miniature tri-axial force sensor for feedback in minimally invasive surgery. In E. Guglielmelli (Ed.), *Proceedings of the 4th IEEE RAS & EMBS International Conference on Biomedical Robotics and Biomechatronics* (pp. 805-810). Rome, Italy: Universita Campus Bio-Medico di Roma.

Bao, J., Xiao, J., Fan, L., Li, X., Hai, Y., Zhang, T., & Yang, C. (2014). All-optical NOR and NAND gates based on photonic crystal ring resonator. *Optics Communications, 329*, 109-112.

Beyeler, F., Neild, A., Oberti, S., Bell, D. J., Sun, Y., Dual, J., & Nelson, B. J. (2007). Monolithically fabricated micro-gripper with integrated force sensor for manipulating microobjects and biological cells aligned in an ultrasonic field. *IEEE/ASME Journal of Microelectromechanical Systems, 16*(1), 7-15.

Boeck, R., Jaeger, N. A. F., Rouger, N., & Chrostowski, L. (2010). Series-coupled silicon racetrack resonators and the Vernier effect: Theory and measurement. *Optics Express, 18*(24), 25151-25157.

Bulutay, C., Turgut, C. M., & Zakhleniuk, N. A. (2010). Carrier-induced refractive index change and optical absorption in wurtzite InN and GaN: Full-band approach. *Physical Review B, 81*(15), 155206.

Cappelleri, D. J., Piazza, G., & Kumar, V. (2011). A two dimensional vision-based force sensor for microrobotic applications. *Sensors and Actuators A: Physical, 171*(2), 340-351.

Caseiro, D., Santos, S., Ferreira, C., & Neves, C. (2014). High sensitivity micro-machined piezoresistive strain sensor. *Procedia Engineering, 87*, 1362-1365.

Chen, Y., Yan, S. C., Zheng, X., Xu, F., & Lu, Y. Q. (2014). A miniature reflective micro-force sensor based on a microfiber coupler. *Optics Express, 22*(3), 2443-2450.

Cho, C., & Ryuh, Y. (2016). Fabrication of flexible tactile force sensor using conductive ink and silicon elastomer. *Sensors and Actuators A: Physical, 237*, 72-80.

Dumeige, Y., Arnaud, C., & Fe´ron, P. (2005). Combining FDTD with coupled mode theories for bistability in micro-ring resonators. *Optics Communications, 250*(4-6), 376-383.

Enikov, E., & Nelson, B. (2000). Three-dimensional microfabrication for a multi-degree-of-freedom capacitive force sensor using fibre-chip coupling. *Journal of Micromechanics and Microengineering, 10*(4), 492-497.

Hopcroft, M. A., Nix, W. D., & Kenny, T. W. (2010). What is the Young's modulus of silicon? *Journal of Microelectro-Mechanical Systems, 19*(2), 229-238.

Jin, W. L., & Mote, C. D. (1998). A six-component silicon micro force sensor. *Sensors and Actuators A: Physical, 65*(2), 109-115.

Kim, J. T. (2015). Silicon optical modulators based on tunable plasmonic directional couplers. *IEEE Journal of Selected Topics in Quantum Electronics, 21*(4), 3300108.

Li, X., Su, D., & Zhang, Z. (2009). A novel technique of microforce sensing and loading. *Sensors and Actuators A: Physical, 153*(1), 13-23.

Liua, C. P., Leea, K. J., Koa, C. H., & Dong, B. Z. (2007). Characteristics of optical multiple channelled filters made of aperiodically patterned phase elements. *Optics and Laser Technology, 39*(2), 415-420.

Ma, Z., & Ogusu, K. (2011). Channel drop filters using photonic crystal Fabry-Perot resonators. *Optics Communications, 284*(5), 1192-1196.

Marchi, G., Stephan, V., Dutz, F. J., Hopf, B., Polz, L., Huber, H. P., & Roths, J. (2016). Femtosecond laser machined micro-structured fiber Bragg grating for simultaneous temperature and force measurements. *Journal of Lightwave Technology, 34*(19), 4557-4563.

Molaei, S. (2016). The measurement of Young's modulus of thin films using secondary laser speckle patterns. *Measurement, 92*, 28-33.

Peirs, J., Clijnen, J., Reynaerts, D., Van Brussel, H., Herijgers, P., Corteville, B., & Boone, S. (2004). A micro optical force sensor for force feedback during minimally invasive robotic surgery. *Sensors and Actuators A: Physical, 115*(2-3), 447-455.

Perez, D., Domenech, D., Munoz, P., & Capmany, J. (2016). Electro-Refraction modulation predictions for silicon graphene waveguides in the 1540-1560 nm region. *IEEE Photonics Journal, 8*(5), 4501613.

Prasad, P. R., Selvaraja, S. K., & Varma, M. M. (2016). Full-Range detection in cascaded microring sensors using thermooptical tuning. *Journal of Lightwave Technology, 34*(22), 5157-5163.

Rabus, D. G. (2002). *Realization of optical filters using ring resonators with integrated semiconductor optical amplifiers in GaInAsP/InP*. (Doctoral thesis). Retrieved from Deposit Once Research Rata and Publications database. (ISBN 3-89959-022-8).

Rabus, D. G., Hamacher, M., Troppenz, U., & Heidrich, H. (2002). Optical filters based on ring resonators with integrated semiconductor optical amplifiers in GaInAsP-InP. *IEEE Journal of Selected Topics in Quantum Electronics, 8*(6), 1405-1411.

Rakshit, J. K., & Roy, J. N. (2014). Micro-ring resonator based all-optical reconfigurable logic operations. *Optics Communications, 321*, 38-46.

Takara, H., Ohara, T., Yamamoto, T., Masuda, H., Abe, M., Takahashi, H., & Morioka, T. (2002). Field demonstration of over 1000-channel DWDM transmission with supercontinuum multi-carrier source. *Electronics Letters, 41*(5), 270-271.

Tan, U. X., Bo, Y., Gullapalli, R., & Desai, J. P. (2011). Triaxial MRI-compatible fiber-optic force sensor. *IEEE Transactions on Robotics, 27*(1), 65-74.

Tokuno, T., Tada, M., & Umeda, K. (2008). High-precision MRI-compatible force sensor with parallel plate structure. In *Proceedings of the 2nd IEEE RAS & EMBS International Conference on Biomedical Robotics and Biomechatronics* (pp. 33-38). Scottsdale, AZ, USA.

Xing, R., & Jian, S. (2017). Numerical analysis on tunable multilayer nanoring waveguide. *IEEE Photonics Technology Letters, 29*(12), 967-970.

Xu, Q., Almeida, V. R., Panepucci, R. R., & Lipson, M. (2004). Experimental demonstration of guiding and confining light in nanometer-size low-refractive-index material. *Optics Letters, 29*(14), 1626-1628.

Yan, X., Ma, C. S., Zheng, C. T., Wang, X. Y., & Zhang, D. M. (2010). Analysis of polymer electro-optic microring resonator switches. *Optics and Laser Technology, 42*(3), 526-530.

Yang, J., Zhou, Q., Zhao, F., Jiang, X., Howley, B., Wang, M., & Chen, R. T. (2003). Characteristics of optical bandpass filters employing series-cascaded double-ring resonators. *Optics Communications, 228*(1-3), 91v98.

Yupapin, P. P., & Suwancharoen, W. (2007). Chaotic signal generation and cancellation using a micro ring resonator incorporating an optical add/drop multiplexer. *Optics Communications, 280*(2), 343v350.

Zadeh, E. G., Charca, G. A., Gholamzadeh, B., Ghasemi, S., & Magierowski, S. (2017). Towards scalable capacitive cantilever arrays for emerging biomedical applications. *Sensors and Actuators A: Physical, 260*, 90-98.